Atmospheric Research 313 (2025) 107757

Contents lists available at ScienceDirect

Atmospheric Research

journal homepage: www.elsevier.com/locate/atmosres

Understanding heavy precipitation events in southern Israel through atmospheric electric field observations

Roy Yaniv [a,b,*], Yoav Yair [c], Assaf Hochman [a]

[a] Fredy and Nadine Herrmann Institute of Earth Sciences, The Hebrew University of Jerusalem, Israel
[b] Gertner Institute, Climate Center, Sheba Medical Center, Ramat Gan, Israel
[c] School of Sustainability, Reichmann University, Herzliya 4610101, Israel

ARTICLE INFO

Keywords:
Potential Gradient
Extreme weather
Lightning
Cyclone
Synoptic classification

ABSTRACT

Characterizing the interaction between meteorological variables such as humidity, wind speed, cloud cover, and precipitation with the atmospheric electric field is vital for improving the nowcast of extreme weather events such as heavy precipitation. With this aim, we provide minute-scale electric field observations in southern Israel. These were taken during low-pressure weather systems in winter, often termed 'Cyprus Lows.' We focus only on precipitating ('wet') events, where rain was measured at the surface during and after the cold front's passage. The mean |PG| values for 'wet' Cyprus Lows are higher (Hundreds to thousands V m^{-1}) compared with the mean fair-weather values (~100–200 V m^{-1}, and exhibit a sharp and rapid increase of the |PG| of up to tens of V m^{-1} min^{-1} during the arrival of the cold front and hundreds of V m^{-1} min^{-1} during precipitation. Then, we analyzed selected case studies in detail. The response of the |PG| to thunderstorm clouds, i.e., Cumulonimbus, is an increase to values of thousands of V m^{-1}. The temporal evolution of the |PG| allowed us to identify the type of cloud and its life cycle stage. We suggest that using state-of-the-art 1 Hz measurements of the |PG| and deducing cloud patterns at strategic locations, such as in arid regions like southern Israel, may improve the nowcasting capabilities of localized heavy precipitation events.

1. Introduction

The atmospheric Potential Gradient (or PG) is crucial in studying Earth's global electrical circuit. Previous studies have demonstrated that the global distribution of lightning activity and shower clouds influences the PG. One well-known example is the 'Carnegie curve,' which is a century-old representation of the diurnal variation of the PG at the surface under fair weather conditions, with values ranging from 100 to 300 V m^{-1} (Torreson et al., 1946; Israël, 1970; Rycroft et al., 2008; Rycroft et al., 2012; Harrison, 2013; Harrison and Nicoll, 2018).

Various natural meteorological and anthropogenic conditions influence the PG. These include dust storms, snow, pollution, clouds, fog, variations in wind speed, and relative humidity. A plethora of studies have reported significant variations in PG values, ranging up to thousands of volts per meter for dust events, hundreds of volts per meter for fog and pollution events, and tens of volts per meter for cloud events with no precipitation (Aplin, 2012; Nicoll and Harrison, 2016; Yair et al., 2016; Yaniv et al., 2016, 2017; Yair et al., 2019; Harrison et al., 2020; Karagioras and Kourtidis, 2021; Kourtidis et al., 2021; Afreen et al., 2022; Nicoll et al., 2022; Yaniv and Yair, 2022,).

Characterizing the interaction between the electric field and precipitation may improve our ability to nowcast heavy precipitation events (Wu et al., 2024) or fog (Yair and Yaniv, 2023; Miller et al., 2024; Harrison and Riddick, 2024). Previous studies have reported that rain carries a charge, causing vertical current (up to 1000 × 10^{-15} A cm^{-2}), which produces electric fields. The assumption was that the higher the rain rate, the stronger the currents were (Simpson, 1910; Chalmers, 1951). However, this hypothesis has not been validated yet. Case studies of rainy events and their effect on the electric field have been analyzed by Takeda et al. (1976) in Japan, Reuveni et al. (2017) in northern Israel, and Karagioras and Kourtidis (2021) in Greece. Results from Japan imply a positive correlation between rain rate and peak electric field values, with PG values reaching up to 700 V m^{-1} for rain rates up to 100 mm h^{-1} (Takeda et al., 1976). Weak rain rates of up to 5 mm h^{-1} and PG enhancements of up to 3500 V m^{-1} were reported by Reuveni et al. (2017). Karagioras and Kourtidis (2021) have reported PG values of up to 5000 V m^{-1} during rain rates of up to 1 mm h^{-1}. Higher rain rates of ~4 mm h^{-1} have shown lower PG values of up to 2000 V m^{-1}.

* Corresponding author at: Fredy and Nadine Herrmann Institute of Earth Sciences, The Hebrew University of Jerusalem, Israel.
E-mail address: roy.yaniv@mail.huji.ac.il (R. Yaniv).

https://doi.org/10.1016/j.atmosres.2024.107757
Received 3 June 2024; Received in revised form 31 October 2024; Accepted 31 October 2024
Available online 6 November 2024

Table 1
'Wet' Cyprus Low events with the following columns: mean |PG| (V m^{-1}), median daily |PG| (V m^{-1}), |PG| difference range Δ|PG| [V m^{-1}], rate of |PG| change Δ|PG|/Δt [V m^{-1} min^{-1}], Δt of the front (minutes), mean Humidity [%], median humidity [%], range of humidity ΔH [%], rate of humidity change ΔH/Δt [% min^{-1}].

Event Date	Mean |PG| [V m^{-1}]	Median |PG| [V m^{-1}]	Δ|PG| [V m^{-1}]	Δ|PG|/Δt [V m^{-1}/min]	Δt (minutes)	Mean Humid [%]	Median Humid [%]	ΔH [%]	ΔH/Δt [%/min]
6–11.1.2014	2059	60	51–15,009	49.8	300	87	86	82–91	0.03
11–13.12.2014	1105	157	193–14,049	54.7	220	62	58	46–86	0.18
5–9.1.2018	839	56	52–15,293	80.2	190	77	77	67–87	0.11

More recent studies have quantified the effect of convective clouds on the electric field. Indeed, the authors have found different electric field responses for each stage of the Cumulonimbus cloud lifetime, i.e., growth stage, mature, and dissipation (Bennett and Harrison, 2007; Pustovalov and Nagorskiy, 2018a, 2018b). We refer to the appendix for a reproduced figure from Pustovalov and Nagorskiy (2018a) of the PG responses, which will be compared to our findings later in this paper (Fig. 4).

During the winter in Israel, rain events are primarily linked with a low-pressure system often termed 'Cyprus Low' because of their mean cyclogenesis region to the west of Cyprus and their transition across the Mediterranean over Cyprus (Alpert et al., 1990). Cyprus Lows typically form during the cooler months, from autumn through spring (Alpert et al., 2004; Hochman et al., 2018). The influence of the system can extend over a larger region, including parts of Turkey, Greece, Israel, and surrounding coastal areas (Alpert et al., 2004). Cyprus Lows are mid-latitude extra-tropical storms lasting ~1–4 days (Osetinsky and Alpert, 2006; Hochman et al., 2019). When cool air is transported from the eastern part of Europe over the warm waters of the Mediterranean Sea, it becomes moist and unstable (Alpert et al., 2004). Over Israel, this is manifested in increased cloud cover, strong winds, and precipitation, ranging from scattered showers to more persistent and heavy rainfall and thunderstorms (Hochman et al., 2019). Almost 90 % of the annual rainfall occurs in Israel between November and March and is associated with Cyprus Lows. Rainfall in the arid south of Israel is determined by the location of the low-pressure minimum center, which dictates the direction of the wind that funnels moisture toward that region (Saaroni et al., 2010).

This study aims to characterize the interconnections between minute-scale ground-based PG measurements and various meteorological variables during Cyprus Low events, including humidity, wind speed, and cloud cover, focusing on precipitation. The manuscript is organized as follows: Section 2 outlines the data used, including in-situ PG measurements, meteorological reanalysis products, and satellite information. Section 3.1 provides a climatological and selected case study view of the interdependence between the electric field and meteorological variables. Section 3.2 characterizes the link between PG values and the life cycle of individual clouds. Finally, Section 4 discusses the main findings and concludes the study.

2. Data and methods

2.1. Field observations and atmospheric data

We base our analysis on in-situ observations of the PG. We used a calibrated CS110 field mill produced by Campbell Scientific Company (http://www.campbellsci.com/cs110-sensor) for electric field measurements at a sampling frequency of 1 Hz. The station's altitude is 850 m above sea level in an arid, rocky area with a typical Mediterranean desert climate of hot and dry summers and cold winters. The average precipitation is 80 mm y^{-1}, mainly from December to February (according to the Israel Meteorological Service). Electric field measurements are available from January 2015 until October 2017. The data is saved locally and uploaded to the GloCAEM database (GLObal Coordination of Atmospheric Electricity Measurements) at Reading University (Nicoll et al., 2019). In addition to the electric field measurements, the Wise Observatory operates an automated meteorological weather station recording various atmospheric variables, including temperature, humidity, pressure, and wind. For a detailed description of the instruments located at the Wise Observatory near Mitzpe Ramon (30°35'N, 34°45'E; Fig. 2D), we refer the reader to Yaniv et al. (2016, 2017).

To understand the influence of aerosols on the PG, we use the AERONET (AErosol RObotic NETwork) ground-based remote sensing aerosol stations established by NASA (Holben et al., 1998). These stations provide globally distributed observations of aerosol parameters, including Aerosol Optical Depth (AOD). The AERONET station in Israel is located in Sede-Boker, approximately 20 km north of the Wise Observatory (30.855 N, 34.782E).

To analyze the atmospheric conditions during precipitation events associated with Cyprus Lows, we produced maps of mean sea level pressure, surface temperature, cloud coverage, and precipitation obtained from the ERA5 reanalysis with hourly temporal resolution and 0.25° x 0.25° grid-spacing (Hersbach, 2016). ERA5 is the state-of-the-art global atmospheric reanalysis product the European Centre for Medium-Range Weather Forecasts (ECMWF) provides.

To analyze single cloud life cycles and their relationship with PG values, we used the cloud product and precipitation data obtained using the Worldview open-source code website (https://worldview.earthdata.nasa.gov/). The Moderate Resolution Imaging Spectroradiometer (MODIS) is a sun-synchronous orbiter that passes once a day (midday) over Israel and combines infrared and visible observations to determine cloud parameters, such as cloud top pressure and temperature, onboard NASA's Terra and Aqua satellites. NOAA's Visible Infrared Imaging Radiometer Suite (VIIRS) uses radiometric bands covering wavelengths from 0.41 to 12.5 μm on board the Suomi National Polar-Orbiting Partnership (Suomi NPP) spacecraft. It provides cloud optical thickness and cloud top height data. In addition, we used the Integrated Multi-satellite Retrievals for the Global Precipitation Mission (IMERG) algorithm, combining information from the Global Precipitation Mission (GPM) satellite constellation providing precipitation rates.

2.2. Classification of 'wet' events associated with Cyprus Lows

We employ the semi-objective synoptic classification algorithm developed by Alpert et al. (2004) and upgraded in Ludwig and Hochman (2022). This classification effectively represents the regional hydroclimate conditions in the Eastern Mediterranean, with a particular emphasis on Cyprus Lows, which are central to this study (Saaroni et al., 2010; Shalev et al., 2011; Dayan et al., 2012; Hochman et al., 2018). The algorithm utilizes daily mean surface air temperature, sea level pressure, and 500 hPa geopotential height fields from the ERA5 reanalysis data for the Eastern Mediterranean region (27.5°N–37.5°N; 30°E–40°E). The reader is referred to Alpert et al. (2004) for further details.

Following the classification of Cyprus Low events, we selected several events during 2014–2020 when electric field and weather observations were readily available from the Wise Observatory station (see Section 2.1). These events were further classified into 'wet' events since

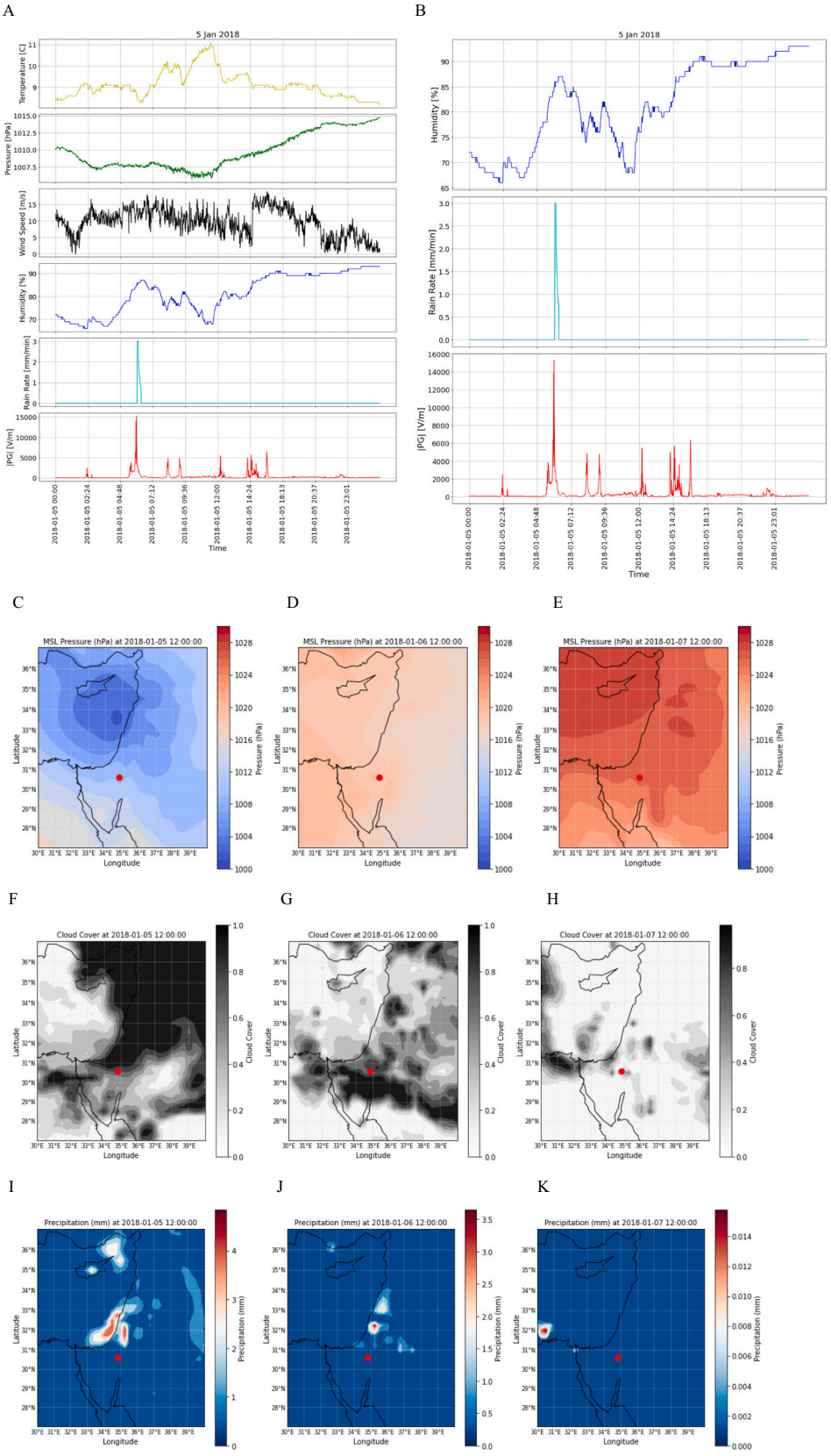

Fig. 1. A Cyprus Low event on 5–10 January 2018. – (A) |PG| in V m^{-1} and weather parameters from 5 January 2018 (B) Zoom-in on the Humidity, Rain rate, and |PG| on 5 January, (DEF) ERA5 reanalysis data of Mean Sea Level Pressure in Pa of the entire event, (GHI) cloud coverage, and (JKL) total precipitation in mm. The highest peak in the |PG| on 5 January (A) corresponds to the passage of convective clouds with the electric field signature and will be covered in detail later in the paper. Red dots are the locations of the CS110 *E*-field mill. (For interpretation of the references to colour in this figure legend, the reader is referred to the web version of this article.)

Table 2
Eight days of rain events with maximum daily |PG| recorded during rainfall.

Date	Precipitation Rate [mm min^{-1}]	Max |PG|	Date	Precipitation Rate [mm min^{-1}]	Max |PG|
2014-01-10	10	15,706	2018-01-27	4.5	8210
	13	15,628		1	6150
2014-02-16	5	17,635	2018-02-13	2	5033
	2.5	17,364		5	4598
2018-01-05	3	15,293	2018-02-23	8	13,479
2018-01-06	12	2500		2	8807
2018-01-19	1.2	11,853		8.5	6210

there was measurable precipitation at the site.

3. Results

3.1. The arrival of a 'wet' cold front of Cyprus Lows and the potential gradient response

First, we study the relationship between the electrical response at ground level and various meteorological variables (Table 1 and Fig. 1) of the Cyprus Low. The measured electric field values were transformed to the magnitude of the Potential Gradient (|PG|) throughout the paper ($PG = -Ez$). Cyprus Lows are subject to variations in humidity and different cloud heights, i.e., low, alto, and high in southern Israel during the arrival of the cold front. Indeed, precipitation often occurs over northern and central Israel but not over the southerly arid regions. This links with the cyclone's location, depth, and the Mediterranean coast's orientation (Enzel et al., 2008; Saaroni et al., 2010).

Fig. 1 provides an example of a 'wet' Cyprus Low event from 5 to 10 January 2018. A low-pressure system over Cyprus is observed, leading to north-western winds from the Mediterranean Sea into southern Israel and the Negev Desert. Fig. 1A shows the weather parameters (temperature, pressure, wind, humidity, rain rate) and |PG| indicating the drop in pressure and the increase of moisture and wind speed. This low-pressure system moves eastward according to the pressure maps (Fig. 1CDE), accompanied by a low cloud base, at altitudes ranging from 800 to 1600 m, advancing from the coastal area toward southern Israel in the morning hours till noon time (Fig. 1FGH). The passage of extensive convective clouds over the station resulted in notable peaks in the atmospheric |PG| (Fig. 1A) from 3:00 to 15:00 on 5 January 2018. One of these clouds precipitated over the station (Fig. 1A and 1IJK), as indicated by the peak of 15 k V m^{-1} (Fig. 1A), which will further be analyzed (See Section 3.2 and Fig. 3D). Fig. 1B shows a zoom-in on the arrival of the front, i.e., the time of the increase of humidity (H) and the precipitating cloud. The Δt is the time interval of the of the passage of the cold front reflecting the rise in humidity (H) from the lower humidity value to the higher humidity value (190 min), ranging from 67 % to 87 % with a rate ΔH/Δt of 0.11 [% min^{-1}]. The average |PG| increase rate Δ|PG|/Δt is 80.2 [V m^{-1} min^{-1}] with a mean |PG| value of 839 V m^{-1} and median |PG| value of 56 V m^{-1}.

Two more 'wet' Cyprus Lows case studies are shown in Table 1, displaying broadly similar humidity and |PG| range results during the front entrance. We remind the reader that the daily mean |PG| fair-weather value at the Wise Observatory is 186 V m^{-1} (Yaniv et al., 2016) and that humidity is a factor that causes an increase of ~hundreds of V m^{-1} above fair-weather values during times of ≥95 % (Yaniv et al., 2016; Yair and Yaniv, 2023). The higher values of |PG| in these events are due to low cloud base height and high humidity (Fig. 1B and FGH) and the electric charge carried by the rain droplets (see Section 3.2). These contribute to the overall |PG| values, which are affected by the absence or presence of different types of clouds, especially the charged low ones (Harrison et al., 2020; Yaniv and Yair, 2022).

3.2. The impact of precipitation on potential gradient values

Depending on available data, we analyzed eight rain events (Table 2 and Figs. 2) at the Wise Observatory. The weather station recorded data on rain rate (mm min^{-1}) and ground level |PG|.

Fig. 2A-D presents examples showing the substantial increase in the |PG| values due to direct rain on the station. There is a positive correlation between the |PG| and the occurrence of rain; the |PG| increases dramatically up to ~18 kV m^{-1} under direct rain, but we can see that there is no correlation between the magnitude of the rain rate and the increase in the |PG| as seen from the results in Table 2. We see high rain rates (>5 mm min^{-1}) associated with |PG| variations of 2.5–15 kV m^{-1} and low rain rates (<5 mm min^{-1}) accompanied by |PG| variations of 6–17 kV m^{-1}.

Other |PG| peaks were not associated with direct rainfall but with the passage of electrified convective clouds at different life stages (see Fig. 4). The range of |PG| values due to direct rainfall at the site was a mean of 10,604 V m^{-1} ranging from 2500 to 17,000 V m^{-1}. None of the signals were associated with lightning discharges. Lightning was excluded by mapping lightning strike occurrences using data from the lightning detection system of the Israeli Electric Corporation (Shalev et al., 2011).

The rain event of 5 January 2018 was associated with a deep Cyprus Low system (Fig. 3A), with convective and non-precipitating shower clouds covering almost the entire region (Fig. 3B). The AERONET AOD values indicated aerosol contribution to the |PG| increase (Fig. 3E). The measured aerosol values during the events were compared to fair weather values, with the threshold for AOD aerosol fair weather values in Mitzpe Ramon set at 0.3 to neglect the dust factor as a dominant one (Yaniv et al., 2016; Yair et al., 2016). Previous studies have shown a |PG| increase of up to 2000 V m^{-1} during dust outbreaks with AOD values higher than 1.5–2 (Yair et al., 2016; Katz et al., 2018). Fig. 3E shows AOD product level 1 values of fine and large particles in the range of 0.4–0.7, which are slightly above the fair-weather threshold. Fig. 3D is a zoom-in on the rain peak during the front (Fig. 1B) and shows high values of humidity (78–87 %), the rain rate (up to 3 mm min^{-1}), and the |PG| variations (up to 15,500 V m^{-1}). The Δ|PG|/Δt of the event is 764.5 V m^{-1} min^{-1}, indicating the strong and fast response of the |PG| to rainfall. The event is accompanied by increased cloudiness and thick charged clouds, high relative humidity, and a change in wind direction and intensity (Fig. 1A). In essence, this is not like the suggestion to use |PG| increase as a predictor of fog (Yair and Yaniv, 2023; Nelli et al., 2024). The increase of the AOD (Fig. 3E) in the morning hours correlates with the increase in the wind speed. Katz et al. (2018) reported a |PG| increase of a few hundred

V m^{-1} when AOD values reached ≥3. The measured values during the reported case study are well below, and their |PG| response is negligible compared to the thousands of V m^{-1} responses from the convective front. The |PG| behavior exhibits multiple peaks (marked A-G), with the strongest signal (B) reaching up to 16,000 V m^{-1} and associated with a rain rate of up to 3 mm min^{-1} (Fig. 3D).

While Table 1 summarizes the results of the entire cold front, Table 3

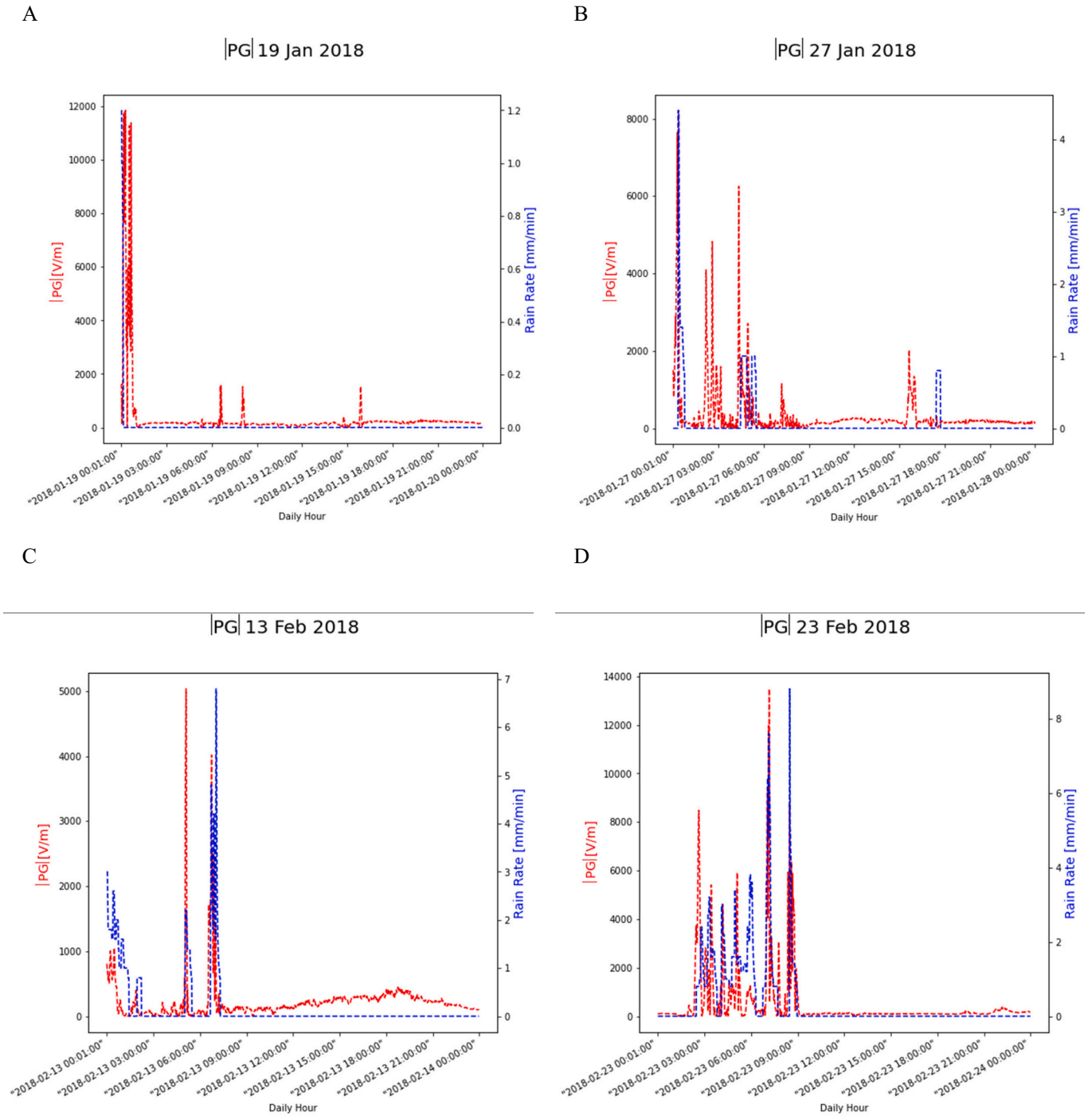

Fig. 2. Example of rain events showing the rain rate in mm min^{-1} (in blue) and the |PG| values in V m^{-1} (in red) from 19 January, 27 January, 13 February, and 23 February 2018 (top row). |PG| has an average value of 10,604 V m^{-1} ranging from 2500 to 17,000 V m^{-1}. (For interpretation of the references to colour in this figure legend, the reader is referred to the web version of this article.)

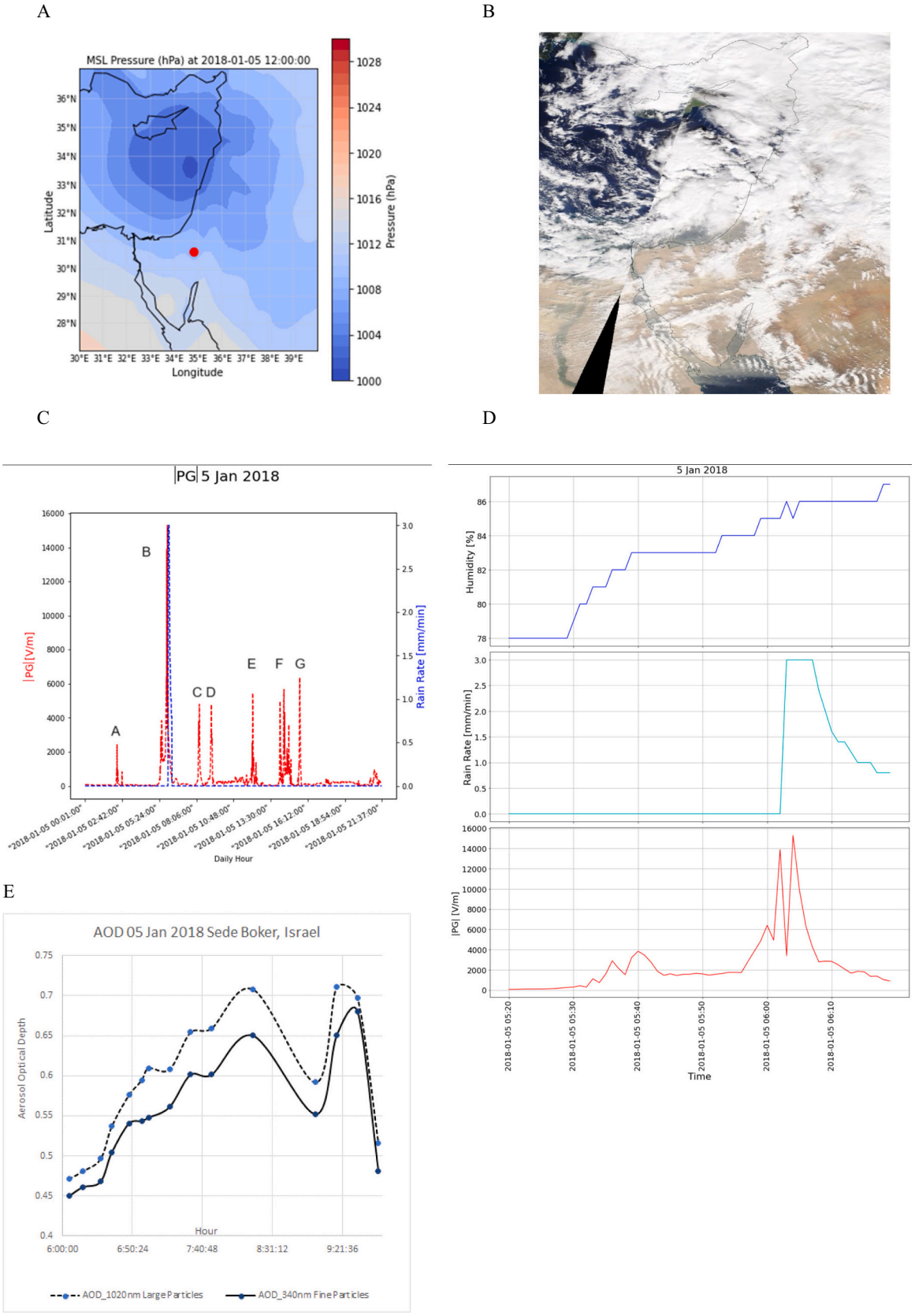

Fig. 3. A rain event on 5 January 2018 linked with a deep Cyprus Low (A). Deep convective clouds over Israel during midday (B). High peaks of |PG| accompanied by rain rate measurements and the passage of convective clouds (C). The relative humidity, rain rate, and |PG| (D) and the Aerosol Optical Depth, which is measured at the Sede Boker station (E).

Table 3
'Wet' Cyprus Low events with the following columns: rate of |PG| change Δ|PG|/Δt [V m^{-1} min^{-1}], Δt of the precipitation (minutes).

	Event Date	Rain Period Δt (minutes)	Δ|PG|/Δt [V m^{-1}/min]
Percipitation	6–11.1.2014	30	500.3
	11–13.12.2014	20	701.8
	5–9.1.2018	20	764.5

depicts a detailed minute-scaled analysis of the peak of the precipitation associated with the three 'wet' Cyprus Low events. We observe a steep increase to high |PG| values in a short period with a Δ|PG| rate of hundreds of V m^{-1} min^{-1}.

3.3. Characterizing the life cycle of single clouds using the potential gradient

We further analyzed other electric field maxima, which were found to be associated with convective non-precipitating clouds or drizzle at different stages passing over the station and are consistent with previously published measurements (Fig. 4; Bennett and Harrison, 2007; Pustovalov and Nagorskiy, 2018a, 2018b). The passage of clouds above the station induces strong electric field variations with an average time scale of 10–15 min. The rain period (Fig. 4B) depicts the stronger values (up to 16 V m^{-1}), and the pattern agrees with past observational and model results (Bennett and Harrison, 2007). The other stages (Dissipation, growth, and early steps) however, reached values of several thousand V m^{-1}.

4. Discussion and conclusions

We characterized the relationship between electric field measurements in the Negev Desert, southern Israel, and various meteorological variables during low-pressure systems in winter, often termed 'Cyprus Lows.'

Analysis of Cyprus Low events revealed significant humidity and cloud coverage variations in the studied region. The mean |PG| values during 'wet' events were significantly higher (up to 16 kV m^{-1}) when compared to results from fair weather, cloudiness, and fog values (Yaniv et al., 2016; Yaniv and Yair, 2022; Yair and Yaniv, 2023) indicating the influence of rain rates, humidity, and heavy cloud cover on |PG| values. Low Cloud act as resistors in the Global Electrical Circuit (Rycroft et al., 2008; Rycroft and Harrison, 2012; Baumgaertner et al., 2014), as they increase columnar resistance of the air due to cloud particles attaching to free ions, hence increasing the surface |PG|.

Our analysis of rain events showed a substantial |PG| increase during 'wet' events, with values reaching 16,000 V m^{-1}. This highlights the role of rain in enhancing the Potential Gradient, likely due to the substantial charge transfer to the ground during rainfall (Chauzy and Despiau, 1980; Soula et al., 2003). Interestingly, while significant Potential Gradient enhancements were observed with rain events, we found no consistent correlation between the rain rate and the Potential Gradient magnitude. This suggests that factors other than rain intensity, such as the type of precipitation and the rain droplets' electrical properties, might influence the electric field as droplets carry charge (more often positive than negative; Soula and Chauzy, 1997) that leads to a complex behavior of the |PG| at the surface, which may weaken or reverse its polarity. Understanding these properties was out of the scope of the present study and will be addressed in future ones.

The passage of convective clouds resulted in notable peaks in the |PG|. Convective clouds precipitating over the station led to further |PG| enhancements. We quantified the increase of the |PG| to thousands of V m^{-1}, with typical values ranging between 2 and 7 kV m^{-1} from the usual fair-weather values of ~100–200 V m^{-1}. Finally, we identified convective clouds and their unique polarity patterns and can characterize their life-cycle stage. Indeed, lower effects on the |PG| from non-shower clouds (alto, cirrus) are negligible since their |PG| variations (~10 V m^{-1}) are too small compared to the precipitating and non-precipitating convective shower clouds (Yaniv and Yair, 2022).

We note that winter clouds in Israel are Cumulonimbus at various stages of development, while the clouds in the UK are also stratiform (Nimbostratus). The charge structure of developing and mature Cb would be a normal dipole and may include a low positive charge center (see Williams, 1989). Stratiform clouds, on the other hand, are likely to display a normal polarity structure, with a positive charge above a negative charge (Nicoll and Harrison, 2016; Harrison et al., 2020). The total charge in convective clouds is expected to be much larger compared with stratiform clouds, so the effects on the |PG| at the surface would be different in magnitude and polarity.

As a caveat, we note that although we analyzed a few selected case studies in detail, our analysis is limited by the number of 'wet' events recorded in a mostly arid region, including electric field measurements.

Overall, the study highlights the critical role of electric measurements in understanding extreme weather events. The data from southern Israel suggests that electric field variations may serve as valuable indicators of impending severe weather events, but additional analysis is required to ascertain this statement. This is particularly true for regions located on the boundary of desert areas, where small lateral distances may be susceptible to large differences in weather and precipitation regimes. Indeed, in the studied area, tiny variations in the location of the low-pressure system may inflict very different atmospheric conditions and weather (Saaroni et al., 2010). Future analysis of this dataset will delve deeper into the electric signals to understand cloud structure and the possibility of predicting rain using such strong variations in the derivative of the PG (e.g., Wu et al., 2024). We, therefore, conclude that implementing cloud-pattern measurements during growth and early mature stages of the electric field at strategic locations may significantly enhance extreme weather nowcasting capabilities in Israel and other sensitive regions in providing in-situ warning to the possible occurrence flash floods. This will ultimately contribute to better preparedness for weather extremes in a changing climate.

CRediT authorship contribution statement

Roy Yaniv: Writing – original draft, Visualization, Software, Methodology, Investigation, Formal analysis, Data curation. **Yoav Yair:** Writing – review & editing, Funding acquisition. **Assaf Hochman:** Writing – review & editing, Supervision, Funding acquisition.

Declaration of competing interest

The authors declare the following financial interests/personal relationships which may be considered as potential competing interests:

Yoav Yair reports financial support was provided by Israel Science Foundation. Assaf Hochman reports financial support was provided by Israel Science Foundation. Assaf Hochman reports financial support was provided by Israel Ministry of Innovation Science & Technology. Assaf Hochman reports financial support was provided by Pazi Foundation. If there are other authors, they declare that they have no known competing financial interests or personal relationships that could have appeared to influence the work reported in this paper.

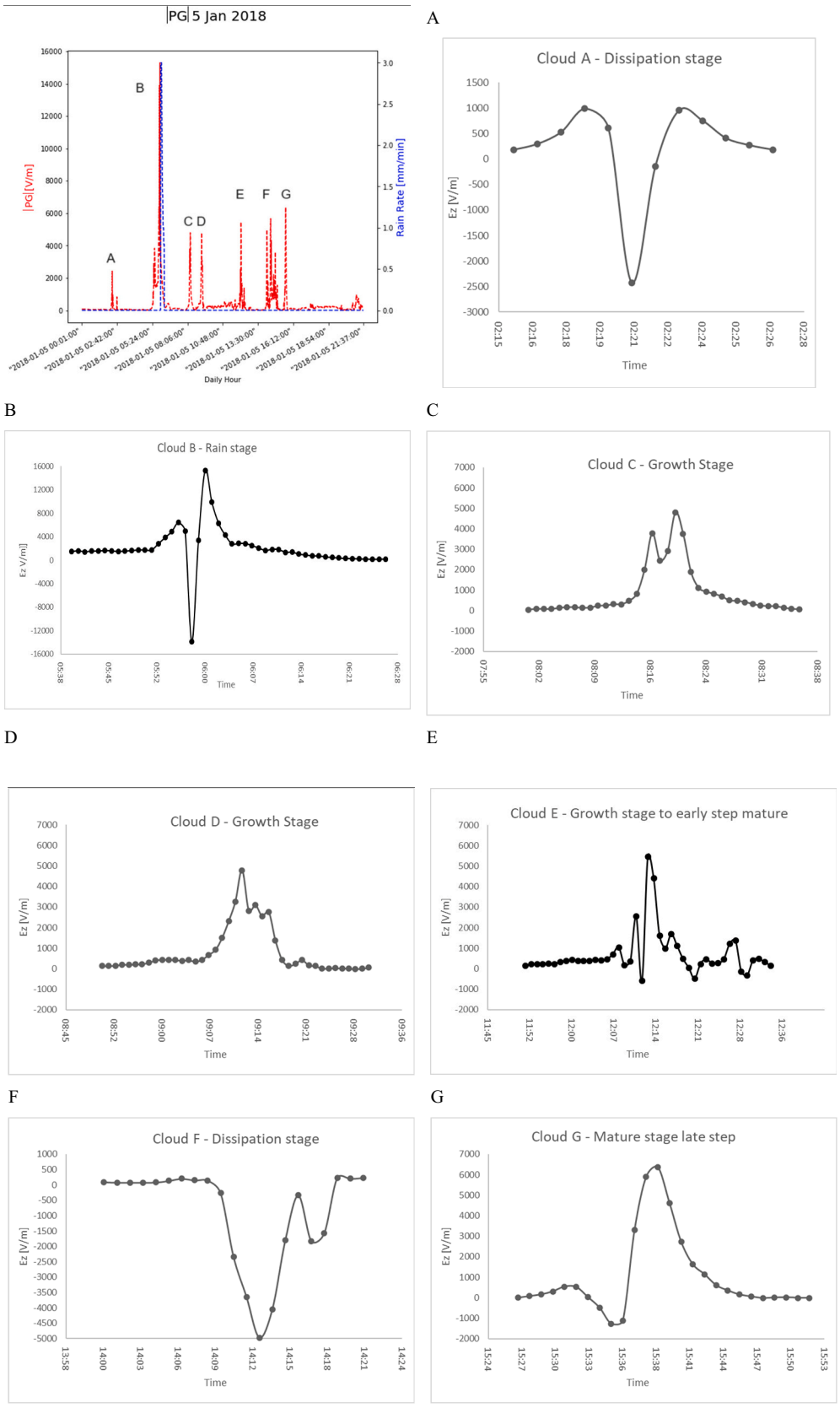

Fig. 4. Electric field (V m^{-1}) of Cumulonimbus convective clouds during their passage over the station at dissipation stage ~02:20 (A), precipitation stage ~6:00 (B), Growth stage ~8:15 (C), ~9:00 (D) and ~ noon (E), dissipation stage ~14:05 (F) and mature stage late step ~15:35 (G).

Acknowledgments

This research was primarily supported by the Israel Science Foundation grant number. 1848/20. The Israel Science Foundation (Grant Number 978/23), the Ministry of Science, Innovation, and Technology of Israel (Grant #4749), and the Pazi Foundation (Grant #434) funded the contribution of RY and AH. The COST Action CA19109 'MedCyclones' and CA22162 'FutureMed', supported by COST (European Cooperation in Science and Technology), support the contribution of AH and RN.

We thank the AeroNet Sede Boker PI Arnon_Karnieli for allowing the use of their data and the Israel Meteorological Service for providing meteorological data. We acknowledge the use of imagery from the NASA Worldview application (https://worldview.earthdata.nasa.gov), which is part of the NASA Earth Observing System Data and Information System (EOSDIS). We thank Mr. Sami Ben-Gigi from Tel-Aviv University's Wise Observatory for his continued technical support.

Appendix A. Appendix

Electric field patterns feature the electric field variations during the passage of Cumulonimbus clouds at various stages, i.e., growth, maturity, and dissipation, which agree with past studies. The patterns are reproduced from Pustovalov and Nagorskiy, 2018a.

Data availability

Data will be made available on request.

References

Afreen, S., Victor, N.J., Nazir, S., et al., 2022. Fair-weather atmospheric electric field measurements at Gulmarg, India. J. Earth Syst. Sci. 131, 7. https://doi.org/10.1007/s12040-021-01745-5.

Alpert, P., Neeman, B.U., Shay-El, Y., 1990. Climatological analysis of Mediterranean cyclones using ECMWF data. Tellus A 42 (1), 65–77.

Alpert, P., Osetinsky, I., Ziv, B., Shafir, H., 2004. Semi-objective classification for daily synoptic systems: Application to the eastern Mediterranean climate change. Int. J. Climatol. 24 (8), 1001–1011.

Aplin, K.L., 2012. Smoke emissions from industrial western Scotland in 1859 inferred from Lord Kelvin's atmospheric electricity measurements. Atmos. Environ. 50, 373–376.

Baumgaertner, A.J.G., Lucas, G.M., Thayer, J.P., Mallios, S.A., 2014. On the role of clouds in the fair weather part of the global electric circuit. Atmos. Chem. Phys. 14 (16), 8599–8610. https://doi.org/10.5194/acp-14-8599-2014.

Bennett, A.J., Harrison, R.G., 2007. Atmospheric electricity in different weather conditions. Weather 62 (10), 277–283.

Chalmers, J.A., 1951. The origin of the electric charge on rain. Q. J. R. Meteorol. Soc. 77 (332), 249–259.

Chauzy, S., Despiau, S., 1980. Rainfall rate and electric charge and size of raindrops of six spring showers. J. Atmos. Sci. 37, 1619–1627.

Dayan, U., Tubi, A., Levy, I., 2012. On the importance of synoptic classification methods with respect to environmental phenomena. Int. J. Climatol. 32 (5), 681–694.

Enzel, Yehouda, et al., 2008. The climatic and physiographic controls of the eastern Mediterranean over the late Pleistocene climates in the southern Levant and its neighboring deserts. Glob. Planet. Chang. 60 (3–4), 165–192.

Harrison, R.G., 2013. The Carnegie curve. Surv. Geophys. 34, 209–232.

Harrison, R.G., Nicoll, K.A., 2018. Fairweather criteria for atmospheric electricity measurements. J. Atmos. Sol. Terr. Phys. 179 (239–250), 2018.

Harrison, R.G., Riddick, J.C., 2024. Atmospheric electricity observations at Eskdalemuir Geophysical Observatory. Hist. Geo Space Sci. 15 (1), 5–16.

Harrison, G., Nicoll, K.A., Mareev, E., Slyunyaev, N., Rycroft, M.J., 2020. Extensive layer clouds in the global electric circuit: their effects on vertical charge distribution and storage. Proc. R. Soc. A 476, 20190758.

Hersbach, H., 2016, December. The ERA5 atmospheric reanalysis. In: AGU Fall Meeting Abstracts, vol. 2016 pp. NG33D-01.

Hochman, A., Harpaz, T., Saaroni, H., Alpert, P., 2018. Synoptic classification in 21st century CMIP5 predictions over the Eastern Mediterranean with focus on cyclones. Int. J. Climatol. 38 (3), 1476–1483.

Hochman, A., Alpert, Harpaz T., Saaroni, H., Messori, G., 2019. A new dynamical systems perspective on atmospheric predictability: Eastern Mediterranean weather regimes as a case study. Sci. Adv. 5, eaau0936. https://doi.org/10.1126/sciadv.aau0936.

Holben, B.N., Eck, T.F., Slutsker, I.A., Tanré, D., Buis, J.P., Setzer, A., et al., 1998. AERONET—A federated instrument network and data archive for aerosol characterization. Remote Sens. Environ. 66 (1), 1–16.

Israël, H., 1970. Atmospheric electricity: Atmosphèarische Elektrizitèat. In: Israel Program for Scientific Translations, vol. 29. US Dept. of Commerce, National Technical Information Service, Springfield, Va.(Jerusalem). Available from the.

Karagioras, A., Kourtidis, K., 2021. A study of the effects of rain, snow and hail on the atmospheric electric field near ground. Atmosphere 12, 996. https://doi.org/10.3390/atmos12080996.

Katz, S., Yair, Y., Price, C., Yaniv, R., Silber, I., Lynn, B., Ziv, B., 2018. Electrical properties of the 8–12th September, 2015 massive dust outbreak over the Levant. Atmos. Res. 201, 218–225.

Kourtidis, K., Szabóné André, K., Karagioras, A., Nita, I.A., Sátori, G., Bór, J., Kastelis, N., 2021. The influence of circulation weather types on the exposure of the biosphere to atmospheric electric fields. Int. J. Biometeorol. 65 (1), 93–105.

Ludwig, P., Hochman, A., 2022. Last glacial maximum hydro-climate and cyclone characteristics in the Levant: a regional modelling perspective. Environ. Res. Lett. 17 (1), 014053.

Miller, C., Nicoll, K., Westbrook, C., Harrison, R.G., 2024, February. The effect of fog on atmospheric electric fields. J. Phys. Conf. Ser. 2702 (1), 012002. IOP Publishing.

Nelli, N., Francis, D., Fonseca, R., Masson, O., Sow, M., Bosc, E., 2024. First measurements of electric field variability during fog events in the United Arab Emirates. J. Arid Environ. 220, 105096.

Nicoll, K.A., Harrison, R.G., 2016. Stratiform cloud electrification: comparison of theory with multiple in-cloud measurements. Q. J. R. Meteorol. Soc. 142, 2679–2691. https://doi.org/10.1002/qj.2858.

Nicoll, K.A., Harrison, R.G., Barta, V., Bor, J., Brugge, R., Chillingarian, A., Chum, J., Georgoulias, A.K., Guha, A., Kourtidis, K., Kubicki, M., Mareev, E., Matthews, J., Mkrtchyan, H., Odzimek, A., Raulin, J.-P., Robert, D., Silva, H.G., Tacza, J., Yair, Y., Yaniv, R., 2019. A global atmospheric electricity monitoring network for climate and geophysical research. J. Atmos. Sol. Terr. Phys. 184, 18–29. https://doi.org/10.1016/j.jastp.2019.01.003.

Nicoll, K.A., Readle, A., Al Kamali, A., Harrison, R.G., 2022. Surface atmospheric electric field variability at a desert site. J. Atmos. Sol. Terr. Phys. 241, 105977.

Osetinsky, I., Alpert, P., 2006. Calendaricities and multimodality in the Eastern Mediterranean cyclonic activity. Nat. Hazards Earth Syst. Sci. 6 (4), 587–596.

Pustovalov, K.N., Nagorskiy, P.M., 2018a. Response in the surface atmospheric electric field to the passage of isolated air mass cumulonimbus clouds. J. Atmos. Sol. Terr. Phys. 172, 33–39.

Pustovalov, K.N., Nagorskiy, P.M., 2018b. Comparative analysis of electric state of surface air layer during passage of cumulonimbus clouds in warm and cold seasons. Atmos. Ocean. Opt. 31, 685–689.

Reuveni, Y., Yair, Y., Price, C., Steinitz, G., 2017. Ground level gamma-ray and electric field enhancements during disturbed weather: combined signatures from convective clouds, lightning and rain. Atmos. Res. 196, 142–150.

Rycroft, M.J., Harrison, R.G., 2012. Electromagnetic atmosphere-plasma coupling: the global atmospheric electric circuit. Space Sci. Rev. 168, 363–384.

Rycroft, M.J., Harrison, R.G., Nicoll, K.A., Mareev, E.A., 2008. An overview of Earth's global electric circuit and atmospheric conductivity. Sp. Sci. Rev. 137 (1–4), 83–105.

Rycroft, M.J., Nicoll, K.A., Aplin, K.L., Harrison, R.G., 2012. Recent advances in global electric circuit coupling between the space environment and the troposphere. J. Atmos. Sol. Terr. Phys. 90-91, 198–211.

Saaroni, H., Halfon, N., Ziv, B., Alpert, P., Kutiel, H., 2010. Links between the rainfall regime in Israel and location and intensity of Cyprus Lows. Int. J. Climatol. 30 (7), 1014–1025.

Shalev, S., Saaroni, H., Izsak, T., Yair, Y., Ziv, B., 2011. The spatiotemporal distribution of lightning over Israel and the neighboring area and its relation to regional synoptic systems. Nat. Hazards Earth Syst. Sci. 11, 2125–2135. https://doi.org/10.5194/nhess-11-2125-2011.

Simpson, G.C., 1910. On the electricity of rain and snow. Proc. Roy. Soc. Lond. Ser. A 83 (564), 394–404.

Soula, S., Chauzy, S., 1997. Charge transfer by precipitation between thundercloud and ground. J. Geophys. Res. 102 (D10), 11061–11069. https://doi.org/10.1029/97JD00007.

Soula, S., Chauzy, S., Chong, M., Coquillat, S., Georgis, J.F., Seity, Y., Tabary, P., 2003. Surface precipitation electric current produced by convective rains during the Mesoscale Alpine Program. J. Geophys. Res. 108, 4395. https://doi.org/10.1029/2001JD001588, D13.

Takeda, T., Moriyama, N., Iwasaka, Y., 1976. A case study of heavy rain in Owase area. J. Meteorol. Soc. Jpn. Ser. II 54 (1), 32–41.

Torreson, O.W., Parkinson, W.C., Gish, O.H., Wait, G.R., 1946. Ocean atmospheric-electric results (Scientific Results of Cruise VII of the Carnegie during 1928–1929 under command of Captain J. P. Ault, vol 3), vol. 568. Researches of the Department of Terrestrial Magnetism. Carnegie Institution of Washington Publication.

Williams, E.R., 1989. The tripole structure of thunderstorms. J. Geophys. Res. 94 (D11), 13151–13167. https://doi.org/10.1029/JD094iD11p13151.

Wu, J., Zou, Z., Li, Y., Xie, F., 2024. The possibility of rainfall nowcasting using atmospheric electric field. Atmos. Res. 298, 107118.

Yair, Y., Yaniv, R., 2023. The effects of fog on the atmospheric electrical field close to the surface. Atmosphere 14 (3), 549.

Yair, Y., Katz, S., Yaniv, R., Ziv, B., Price, C., 2016. An electrified dust storm over the Negev desert, Israel. Atmos. Res. 181, 63–71.

Yair, Y., Reuveni, Y., Katz, S., Price, C., Yaniv, R., 2019. Strong electric fields observed during snow storms on Mt. Hermon, Israel. Atmos. Res. 215, 208–213.

Yaniv, R., Yair, Y., 2022. Electric field variations caused by low, middle and high-altitude clouds over the Negev Desert, Israel. Atmosphere 13 (8), 1331.
Yaniv, R., Yair, Y., Price, C., Katz, S., 2016. Local and global impacts on the fair-weather electric field in Israel. Atmos. Res. 172, 119–125.
Yaniv, R., Yair, Y., Price, C., Mkrtchyan, H., Lynn, B., Reymers, A., 2017. Ground-based measurements of the vertical E-field in mountainous regions and the "Austausch" effect. Atmos. Res. 189, 127–133.